INDUCED IGNITION DUE TO JET BOUNDARY LAYER

GASL Technical Report # 613

PROJECT 8027

COPY 22

GASL Technical Report # 613

INDUCED IGNITION DUE TO JET BOUNDARY LAYER

By: J. Tamagno

Prepared Under Contract # NAS8-20066

Prepared for

National Aeronautics and Space Administration
George C. Marshall Space Flight Center
Huntsville, Alabama 35812

Prepared by

General Applied Science Labs., Inc.
Merrick & Stewart Avenues
Westbury, L.I., N.Y.

Approved by: L M Nucci

L. M. Nucci
Acting General Manager

July 1966

TABLE OF CONTENTS

LIST OF FIGURES

INDUCED IGNITION DUE TO JET BOUNDARY LAYER

ABSTRACT

A study has been made on the possibility of inducing ignition in a hydrogen-air mixture due to high temperature peaks which may exist in the hypersonic boundary layer along the walls of a hydrogen venting system. The combustible mixture may result from hydogen dumping to the air stream during the atmospheric exit of a launch vehicle utilizing hydrogen in its upper stages.

The flow field associated with the development of the mixing region involving hot gases in the air boundary layer and cold hydrogen, has been studied using analytical and numerical techniques where finite rate chemistry has been coupled with diffusion. Two conditions were selected for the analysis, corresponding to a flight Mach number M=5.4 and flight altitudes of 50,000 ft. and 150,000 ft. The results appear to indicate that for the geometric configuration and flow conditions selected in the study, high temperature regions in the boundary layer of the venting system do not constitute a combustion hazard. The above conclusion may not be applicable to configurations which are very different from those assumed herein, nevertheless the usefulness of the analytical technique employed has been demonstrated and can be applied to other practical configurations.

NOMENCLATURE

a	radius of the venting tube
C_p	specific heat at constant pressure
$\bar{C}_p$	specific heat of mixture at constant pressure
h	static enthalpy per unit mass
H	total enthalpy
J	mechanical equivalent of heat
$k_{f,s}$	forward reaction rate
$k_{b,s}$	backward reaction rate
$K_{c,s}$	equilibrium constant
Le	Lewis number
M	Mach number
N	transformed physical coordinate
P	pressure
Pr	Prandtl number
r	radial distance
R	universal gas constant
T	temperature
u	velocity in axial direction
$\dot{w}$	mass rate of production of species
W	molecular weight
Y	mass fraction of species
δ	boundary layer thickness
ϵ_v	viscosity
ϵ_{H_2}, ϵ_{air}	coefficient relating thickness of boundary layer to radius of venting tube
ν'	stoichiometric coefficients for reactants
ν''	stoichiometric coefficients for products
ρ	density
τ_{ID}	ignition delay
τ_R	reaction time
ψ	stream function as defined by Equation (14)

Subscripts

e	air free stream conditions
j	hydrogen characteristics outside the boundary layer
i	denotes a particular species
w	wall conditions

I. INTRODUCTION

A question of considerable importance during the atmospheric exit of a launch vehicle utilizing hydrogen in its upper stages has been that of the potential combustion hazard associated with the venting of hydrogen into the airstream. One area of concern is the possibility that the resulting hydrogen-air mixture could be ignited in the proximity of the launch vehicle. Such ignition and combustion may result in significant alteration of the heat transfer to the surface of the vehicle and of the aerodynamic forces and moments applied to the vehicle.

The description of the actual phenomena which may be involved in such cases will be complicated and will depend on the mode of injection, the airstream conditions and the characteristics of the dumping hydrogen.

In reference 1 representative modes of hydrogen venting were examined qualitatively in order to establish conditions of velocity, pressure and temperature where combustion might occur. The approach followed in the aforementioned reference was basically connected with the research performed in the kinetics of the hydrogen-air system. In any combustion process two periods may be distinguished; the first is the induction (or ignition delay) period which involves major alterations in composition, but no significant heat release i.e. no temperature rise; the second is the heat release (or reaction) period during which the temperature does rise. The times associated with both periods are readily estimated for a given pressure and initial temperature by means of the following empirical correlations:

$$\tau_{ID} P \simeq 8 \times 10^{-3} \, e^{\frac{9600}{T_i}} \tag{1}$$

$$\tau_R P^{1.7} \simeq 105 \, e^{-1.12 \times 10^{-3} T_i} \tag{2}$$

where times are in microseconds, T_i (initial temperature) in degrees Kelvin and P (pressure) in atmospheres.

It is therefore possible to apply such estimates to determine the flow lengths associated with the induction and heat release periods if the times given by the Equations (1) and (2) are multiplied by a representative flow velocity, and thus to indicate under what flow conditions combustion in the vicinity of the launch vehicle can be expected.

These estimates can be employed to make judgements as to the injection modes leading to the smallest probability of combustion arising in a given exit trajectory. They do not, however, include consideration of such effects as vaporization, mixing and flow interaction which will undoubtedly alter the predicted distances from the ejection point on the launch vehicle to the downstream point where combustion could occur if ignition eventually does take place. It is apparent then, that more realistic studies are desirable where these effects must be included.

This report contains the analysis and the results of calculations which include the effects of mixing in a practical situation where the ejected hydrogen could be ignited by high temperature regions, characteristic of the hypersonic boundary layer along the walls of the venting tube.

II. BOUNDARY LAYER TEMPERATURE DISTRIBUTION

A typical launch trajectory under consideration is shown in Figure 1. This provides the free stream values of velocity and stagnation enthalpy prevailing at the edge of the boundary layer on the wall of the venting tube. Within the approximation of the Prandtl and Lewis numbers equal to unity, the Crocco relation can be applied to relate the enthalpy and velocity distributions in the boundary layer. Accordingly,

$$h = -\frac{u_e^2}{2gJ}\,(u/u_e)^2 + (H_e - H_w)\frac{u}{u_e} + H_w \tag{3}$$

where subscript e denotes free stream conditions.

It is easy to show that the maximum enthalpy within the layer is given by

$$h_{max} = \tfrac{1}{4}(H_e - H_w)^2\,\frac{2gJ}{u_e^2} + H_w = \tfrac{1}{4}(h_e - H_w)^2\,\frac{2gJ}{u_e^2} + \tfrac{1}{2}(h_e + H_w) + \tfrac{1}{4}\left(\frac{u_e^2}{2gJ}\right) \tag{4}$$

The velocity at which this maximum is obtained is given by

$$\frac{u}{u_e} = \frac{H_e - H_w}{2}\,\frac{2gJ}{u_e^2} \tag{5}$$

By using Equation (4) and the Mollier chart for air, the curves of Figures 2 and 3 may be constructed. In these figures, the maximum temperatures which may be found in the boundary layer at different altitude and flight speed were plotted considering two possible values of the wall enthalpy. One corresponds to an adiabatic wall ($H_w = H_e$) and the other to a cold wall with $H_w = h_e$.

It is seen that it is desirable to keep the wall temperature as low as possible in order to reduce the temperature peak in the boundary layer.

If a practical limit of autoignition is fixed at 1000°K, Figures 2 and 3 show that the possibility of inducing combustion due to high temperature peaks in the boundary layer exist only for flight speeds above 4000 ft/sec for an adiabatic wall and only above 8000 ft/sec for

a highly cooled wall.

Equation (3) gives the enthalpy distribution in the boundary layer as a function of the velocity distribution. For a turbulent boundary layer the velocity profiles may be approximated by the

$$u/u_e = (\gamma/\delta)^{1/n} \tag{6}$$

where n may be taken equal to seven.

In the case of a laminar boundary layer the velocity profiles discussed in Reference 2 are employed:

$$u/u_e = A \ln (1+GN) + BN^2 + CN^3 + DN^4 \tag{7}$$

where the coefficients A,B,C and D are determined satisfying appropriate boundary conditions, and where N is related to the physical coordinate through the modified Dorodnitsyn transformation:

$$N=1/\delta_m \int_a^{a+r} \rho/\rho_e \, r\,dr \tag{8}$$

with δ_m taken as

$$\delta_m = \int_a^{a+\delta} \rho/\rho_e \, r\,dr \tag{9}$$

In addition

$$G = \frac{2\delta_m}{a^2} \rho_e/\rho_w \tag{10}$$

where a is the nozzle radius.

The velocity profiles given by (7) are of interest because they may be applied to the case of an axially symmetric flow along a slender body over which the thickness δ of the viscous layer need not be small compared to the body radius. This may be of interest in high altitude flight where thicker boundary layers are expected because of the decreased Reynolds numbers encountered.

III. ANALYSIS

A theoretical analysis of the problem under consideration cannot be performed without defining a suitable model. As discussed previously, the actual phenomena which may be involved in the application of interest will be complicated and will depend on the mode of ejection, the air stream condition and the characteristics of the dumped hydrogen.

Considering that the specific geometric configurations and flow conditions for the fuel exhaust problem were still in the development stage, the calculations presented here merely represent an illustration of the technique for analyzing the possibility of combustion initiation due to nozzle boundary layer effects.

The model used in the theoretical analysis is shown schematically in Fig. 4. It consists of a circular jet of hydrogen exhausting into high speed air. The conditions selected for the numerical analysis correspond to a flight Mach number 5.4 (u_e= 5780 ft/sec) and flight altitudes of 50,000 ft and 150,000 ft. In both cases conservative estimates for combustion initiation were obtained by assuming that the wall of the exhaust tube was at the adiabatic temperature of 1660^{o}K.

In addition, it was assumed that the air boundary layer has a thickness δ of one tenth of the radius of the venting tube which was taken equal to 0.125 ft. The initial velocity and temperature profile inputs are presented in Fig. 5. These profiles were computed considering that the boundary layer was turbulent.

The flow field associated with the development of the mixing region involving the hot gases of the air boundary layer and the cold hydrogen has been studied using analytical and numerical techniques developed at GASL. These techniques depend upon two principal advances. The first, involved the development of numerical "subdomain" methods of analyzing finite-rate chemical systems characterized by many components and many reactions. The second advance involved the coupling of the preceding numerical technique (which is initially a one-dimensional streamline calculation) with two-dimensional and axisymmetric systems. This was carried out by dividing each species mass fraction into two components, one of which satisfied the coupling diffusion equation whereas the other satisfied a one-dimensional coupled chemical growth equation. These numerical methods have resulted in calculation speeds up to two orders of magnitude faster than heretofore available with conventional techniques.

A detailed description of the above numerical and analytical methods as well as stability analysis may be found in Reference 3. The analysis includes the effect of viscosity, heat conduction and diffusion. Boundary layer approximations are assumed in writing the conservation laws and since chemical reactions are considered, the heat released is included in the energy equation. Continuity equations are satisfied for each chemical species and for the mixture.

The equations used in the analysis are summarized below:

Species Continuity

$$\frac{\partial Y_i}{\partial X} = \frac{1}{\psi}\frac{\partial}{\partial \psi}\left(\frac{\epsilon_v}{Pr}\ Le\ \rho u r^2\ \frac{1}{\psi}\frac{\partial Y_i}{\partial \psi}\right) + \frac{\dot{w}_i}{\rho u} \tag{11}$$

Momentum:

$$\frac{\partial u}{\partial X} = -\frac{1}{\rho u}\frac{dp}{dx} + \frac{1}{\psi}\frac{\partial}{\partial \psi}\left[\frac{1}{\psi}\epsilon_v \rho u r^2 \frac{\partial u}{\partial \psi}\right] \tag{12}$$

Energy:

$$\bar{C}_p \frac{\partial T}{\partial \psi} = \frac{1}{\psi}\frac{\partial}{\partial \psi}\left[\frac{\bar{C}_p}{Pr}\ \frac{1}{\psi}\epsilon_v \rho u r^2 \frac{\partial T}{\partial \psi}\right] + \frac{\epsilon_v \rho u r^2}{\psi^2}$$

$$\left[\left(\frac{\partial u}{\partial \psi}\right)^2 + \frac{Le}{Pr}\frac{\partial T}{\partial \psi}\sum_{i=1}^{N} C_{p_i}\frac{\partial Y_i}{\partial \psi}\right] - \frac{1}{\rho u}\sum_{i=1}^{N} h_i \dot{w}_i + \frac{1}{\rho}\frac{dp}{dx} \tag{13}$$

where ψ is the stream function and is related to r by:

$$r^2 = 2\int_0^{\psi} \frac{\psi' d\psi'}{\rho u} \tag{14}$$

Le is the Lewis number, Pr is the Prandtl number, $\bar{C}_p$ is the specific heat at constant pressure for the mixture and ϵ_v is the viscosity.

The reaction process for N distinct species can be described adequately by the set of R simultaneous reactions:

$$\sum_{i=1}^{N} \nu'_{i,s} M_i \underset{k_{b,s}}{\overset{k_{f,s}}{\rightleftharpoons}} \sum_{i=1}^{N} \nu''_{i,s} M_i \quad \begin{cases} i = 1,2, \ldots N \text{ (species)} \\ s = 1,2, \ldots R \text{ (reactions} \end{cases} \tag{15}$$

The net mass rate of production of the species can be written as:

$$\dot{w}_i = W_i \sum_{s=1}^{R} (\nu''_{i,s} - \nu'_{i,s}) \, k_{f,s} \, \rho^{m_s} \prod_{j=1}^{N} \left(\frac{Y_j}{W_j} \right)^{\nu'_{j,s}} \left[1 - \frac{\rho^{n_s}}{K_{c,s}} \prod_{j=1}^{N} \left(\frac{Y_j}{W_j} \right)^{\nu''_{j,s} - \nu'_{j,s}} \right] \tag{16}$$

where

$$m_s = \sum_{j=1}^{N} \nu'_{j,s} \qquad n_s = \sum_{j=1}^{N} (\nu''_{j,s} - \nu'_{j,s})$$

and $k_{f,s}$ is the forward reaction rate corresponding to the s chemical reaction; $K_{c,s} = k_{f,s}/k_{b,s}$ the equilibrium constant; and $k_{b,s}$ the backward reaction rate of the s chemical reaction.

The R chemical reactions taken into consideration are those described in Reference 4 and are listed below:

$$
\begin{aligned}
&1)\quad H + O_2 \rightleftharpoons OH + O\\
&2)\quad O + H_2 \rightleftharpoons OH + H\\
&3)\quad H_2 + OH \rightleftharpoons H + H_2O\\
&4)\quad 2OH \rightleftharpoons O + H_2O\\
&5)\quad H_2 + M \rightleftharpoons 2H + M\\
&6)\quad H_2O + M \rightleftharpoons OH + H + M\\
&7)\quad OH + M \rightleftharpoons O + H + M\\
&8)\quad O_2 + M \rightleftharpoons 2O + M
\end{aligned}
\qquad (17)
$$

The above chemical reactions involve six (6) reacting species, since nitrogen is considered as an inert gas. The concentration of M acting as a third body is considered to be equal to the sum of all seven (7) of the species concentrations.

The reaction rate coefficients are the following:

$$
\begin{aligned}
k_{f,1} &= 3 \times 10^{14}\, e^{-8810/T}\\
k_{f,2} &= 3 \times 10^{14}\, e^{-4030/T}\\
k_{f,3} &= 3 \times 10^{14}\, e^{-3020/T}\\
k_{f,4} &= 3 \times 10^{14}\, e^{-3020/T}\\
k_{f,5} &= 1.85 \times 10^{20} T^{-1} e^{-54,200/T}\\
k_{f,6} &= 9.66 \times 10^{21} T^{-1} e^{-62,200/T}\\
k_{f,7} &= 8 \times 10^{19} T^{-1} e^{-60,600/T}\\
k_{b,1} &= 2.48 \times 10^{13} e^{-660/T}\\
k_{b,2} &= 1.30 \times 10^{14} e^{-2490/T}\\
k_{b,3} &= 1.33 \times 10^{15} e^{-10,950/T}\\
k_{b,4} &= 3.12 \times 10^{15} e^{-12,510/T}\\
k_{b,5} &= 10^{16} \qquad k_{b,7} = 10^{16}\\
k_{b,6} &= 10^{17} \qquad k_{b,8} = 6 \times 10^{14}
\end{aligned}
\qquad (18)
$$

T is the absolute temperature in degrees Kelvin. The rates $k_{f,1}$-$k_{f,8}$ and $k_{b,1}$-$k_{b,4}$ are in units cm^3 $mole^{-1}$ sec^{-1} whereas $k_{b,5}$-$k_{b,8}$ are in cm^6 $mole^{-2}$ sec^{-1}.

The detailed procedure for computing the species growth terms $\dot{w}_i$ in Equations (11), (13) are discussed in Reference 5. These procedures involve linearization of the species growth expressions, making possible the subsequent use of the subdomain method of integration of the species conservation equations instead of the usual Runge-Kutta and Predictor-Corrector methods.

It will be noted that a fundamental parameter in the foregoing analysis is the formulation of the viscosity model and with it the related conductivity and diffusivity. The accurate determination and fundamental specification of these quantities is the goal of a great deal of effort by many workers and is far from resolution. In the jet under consideration two different limiting regions of mixing can be distinguished, in the near field close to the exit of the jet (potential core) the mixing is close to two-dimensional and the half-width of mixing zone is much less than the radius of the venting tube. In the far field the mixing corresponds to that for the usually considered circular jet. Thus a careful specification of $\epsilon_v(x)$ may be analytically complicated, however, in the immediate vicinity of the nozzle which is the region of interest here, $\epsilon_v \sim kx$ can be considered as a convenient and representative assumption. In general, K is related to the flow variables, e.g., density, velocity, and width of the mixing region, but as a first exploratory step, a value of $K = 10^{-3}$ was fixed based on averaging flow conditions across the mixing zone.

In addition to the aforementioned assumptions concerning the formulation of the viscosity model the Plandtl and Lewis number were considered equal to unity.

It is apparent that the flow field in the immediate vicinity of the nozzle has to be considered initially in great detail. Existing computer programs for the analysis of mixing with combustion were unable to accommodate the large number of grid points necessary for proper resolution of this relatively small region of the flow field. Consequently, a modification of the existing numerical technique was required.

In fact, for the cases considered here, it was found that in order to have good resolution in the region of interest, in excess of 1,000 grid points were required from the axis of symmetry. Since this great number of grid points will increase the computation time to such an extent to render it impractical, the numerical technique was modified to overcome this difficulty.

The modification introduced here consists of concentrating the numerical calculations only on the relevant part of the flow field, i.e. the thin mixing region in the vicinity of the nozzle lip. Thus the potential core region which is yet unaffected by diffusion and combustion

is eliminated from the calculation. This is done by "shifting" the physical axis as shown in Figure 6. The axis is shifted to a location just outside the hydrogen boundary layer $\delta_{H_2} = \epsilon_{H_2} a$ where ϵ_{H_2} is a fraction of the jet radius. The region between ψ_1 (the edge of the H_2 boundary layer) and ψ_2 (the edge of the air boundary layer) can now be divided into a feasible number of grid points giving the desired resolution near the nozzle wall. No loss of accuracy occurs provided the lower edge of the mixing region has not affected the flow in the neighborhood of the shifted axis. When the mixing region approaches the fictitious axis, it is shifted downward until it coincides with the physical axis. From this point on, the calculation would proceed in the usual manner. The extent of the relevant region of the flow field assuming the adiabatic wall condition and turbulent boundary layers in given by:

Air Side:

$$\psi_3^2 - \psi_2^2 = -2\epsilon_{air} a^2 u_e \frac{\Gamma_e}{\xi_e^4}\left[\sum_{n=1}^{3}\frac{\xi_e^n}{2n} + \tfrac{1}{2}\log(1-\xi_e)\right] +$$

$$+ 2a^2\epsilon_{air}^2 u_e \frac{\Gamma_e}{\xi_e^{15/2}}\left[-\sum_{n=1}^{7}\frac{\xi_e^{\frac{2n-1}{2}}}{2n-1} + \tfrac{1}{2}\log\frac{1+\sqrt{\xi_e}}{1-\sqrt{\xi_e}}\right] \qquad (19)$$

and

H_2 Side

$$\psi_2^2 - \psi_1^2 = -2\epsilon_{H_2} a^2 u_j \frac{\Gamma_j}{\xi_j^4}\left[\sum_{n=1}^{3}\frac{\xi_j^n}{2n} + \tfrac{1}{2}\log(1-\xi_j)\right] -$$

$$- 2\epsilon_{H_2} a^2 u_j \frac{\Gamma_j}{\xi_j^{15/2}}\left[-\sum_{n=1}^{7}\frac{\xi_j^{\frac{2n-1}{2}}}{2n-1} + \tfrac{1}{2}\log\frac{1+\sqrt{\xi_j}}{1-\sqrt{\xi_j}}\right] \qquad (20)$$

where

$$\xi = \frac{K_1}{H} \quad ; \qquad K_1 = \frac{u^2}{2gJ}$$

$$\Gamma = \frac{7K_2}{H} \quad ; \qquad K_2 = \frac{P\ W\ C_p}{R}$$

and P, is the pressure, W the molecular weight, C_p the specific heat at constant pressure and R the universal gas constant.

IV. RESULTS OF CALCULATIONS AND CONCLUSIONS

Computed temperature distributions are presented in Figures 7 and 8 for the 50,000 ft and 150,000 ft flight altitude cases. It is seen that the static temperature peak in the boundary layer, which can cause ignition, is reduced well below the autoignition limits at short distances from the nozzle exit. The rate of decay of the temperature peak as a function of the downstream distance, is different in both cases, thus at a flight altitude of 150,000 ft a peak value of $400^{o}K$ is obtained at $x = 4.15 \times 10^{-2}$ ft while at 50,000 ft a maximum value of $600^{o}K$ still exists at twice the above distance.

This is consistent with the strong dependence of the chemical reactions with pressure, in fact, the higher the pressure, the greater the amount of heat liberated in a given distance thus, counteracting the tendency of the diffusive process to smooth-out the temperature profiles. An indication of the incipient chemical activity taking place when the hot region of the boundary layer merges with the cold hydrogen being exhausted is provided by Figures 9 and 10 where mass fractions of H_2O, OH and H are plotted. In Fig. 9, typical radial distributions are presented at a given axial distance $x = 8.10^{-3}$ ft, from the exhaust section while in Fig. 10 are shown the maximum values attained for the above species as a function of the axial distance.

These results appear to indicate that even at extreme cases of low flight altitude, e.g., 50,000 ft and flight Mach number M=5.4, the potential combustion hazard associated with the venting of hydrogen from a jet due to high temperature regions on the boundary layer of the venting tubes does not exist. Although the foregoing conclusions apply to the model selected for the study, the usefulness of the analytical technique employed has been demonstrated and can be applied to other practical configurations.

V. REFERENCES

1. Libby, P.A., et al, "Engineering Estimates of Flow Lengths Associated with the Combustion of Hydrogen-air Mixtures During a Launch Trajectory", GASL TR 330, Dec. 1962.
2. Bloom, M.H. and Stieger, M.H., "On Thick Boundary Layers over Slender Bodies with Some Effects of Heat Transfer, Mass Transfer and Pressure Gradient", Int. J. Heat Mass Transfer, Vol. 5 pp. 513-520.
3. Ferri, A., and et al, "Mixing Processes in Supersonic Combustion" J. Soc. Indust. Appl. Math. Vol. 13, No. 1., March 1965.
4. Slutsky, S. and et al, "Supersonic Combustion of Premixed Hydrogen-Air Flows", AIAA Journal, Vol. 3 No. 9, Sept. 1965, pp. 1599-1605.
5. Moretti, G., "A New Technique for the Numerical Analysis of Non-Equilibrium Flows", AIAA J. 3, 223-229 (1965).

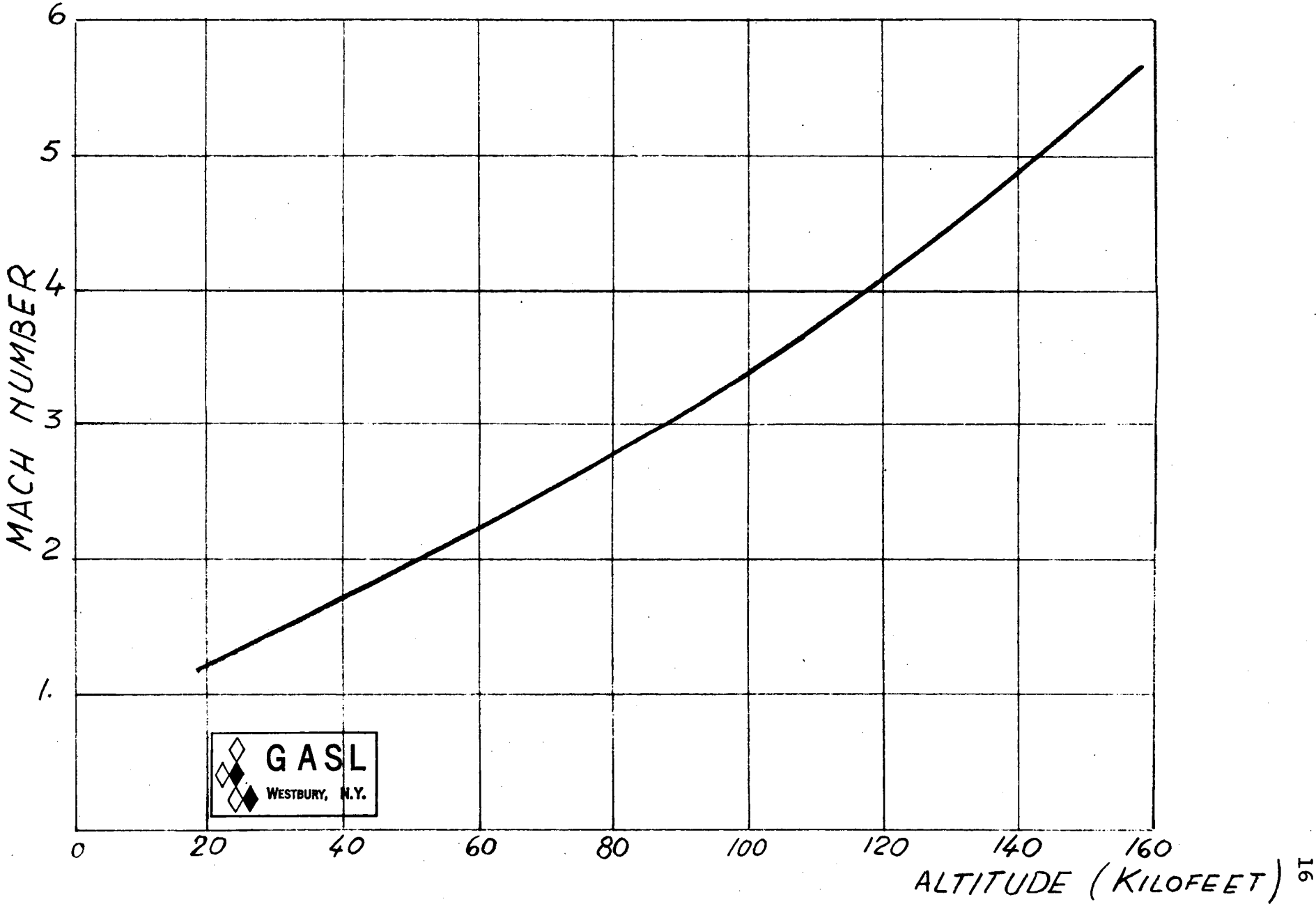

FIG. 1 : FLIGHT CONDITIONS FOR LAUNCH TRAJECTORY

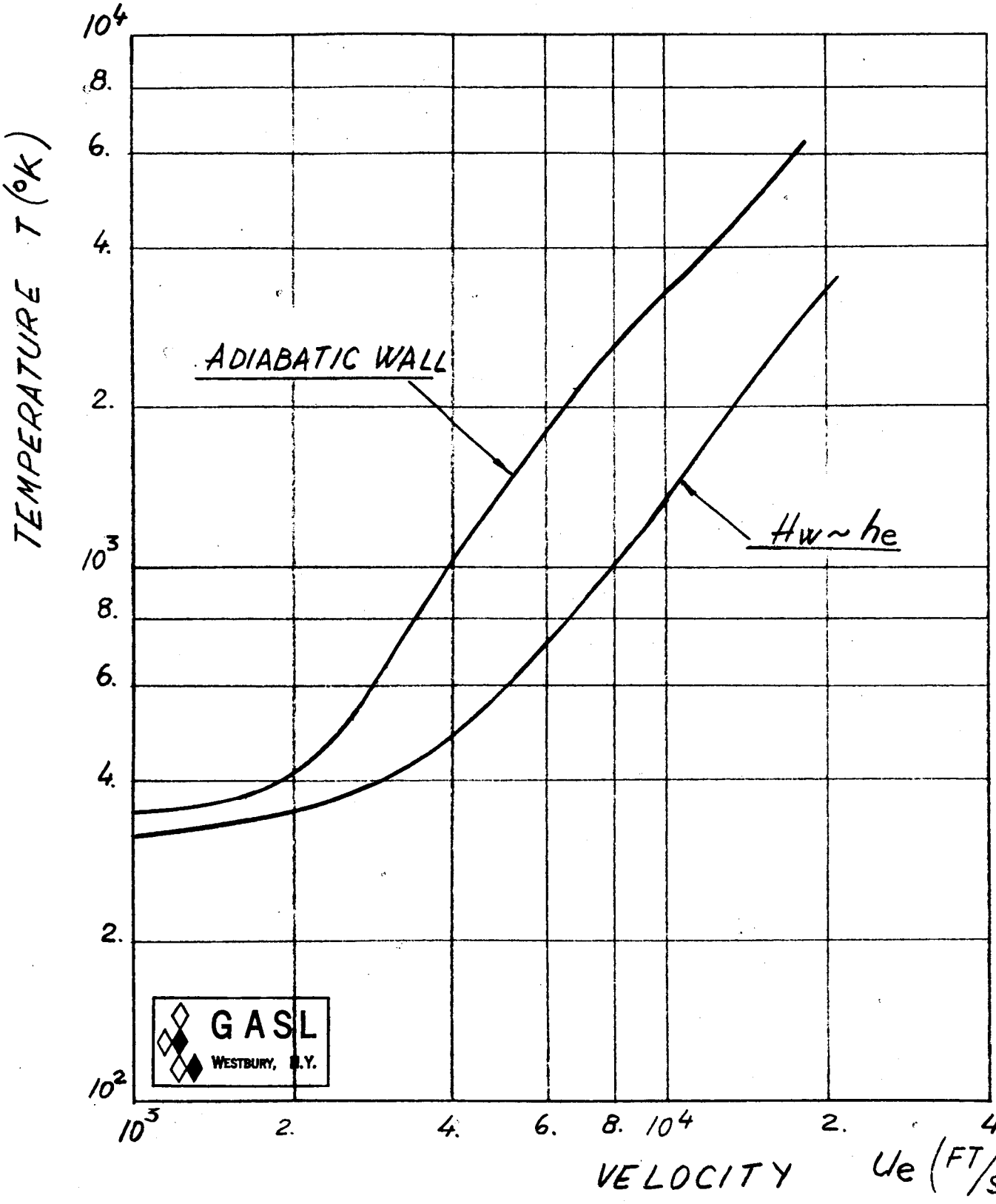

FIG. 2 : MAXIMUM STATIC TEMPERATURE IN THE BOUNDARY LAYER. ALT. : 0 FT

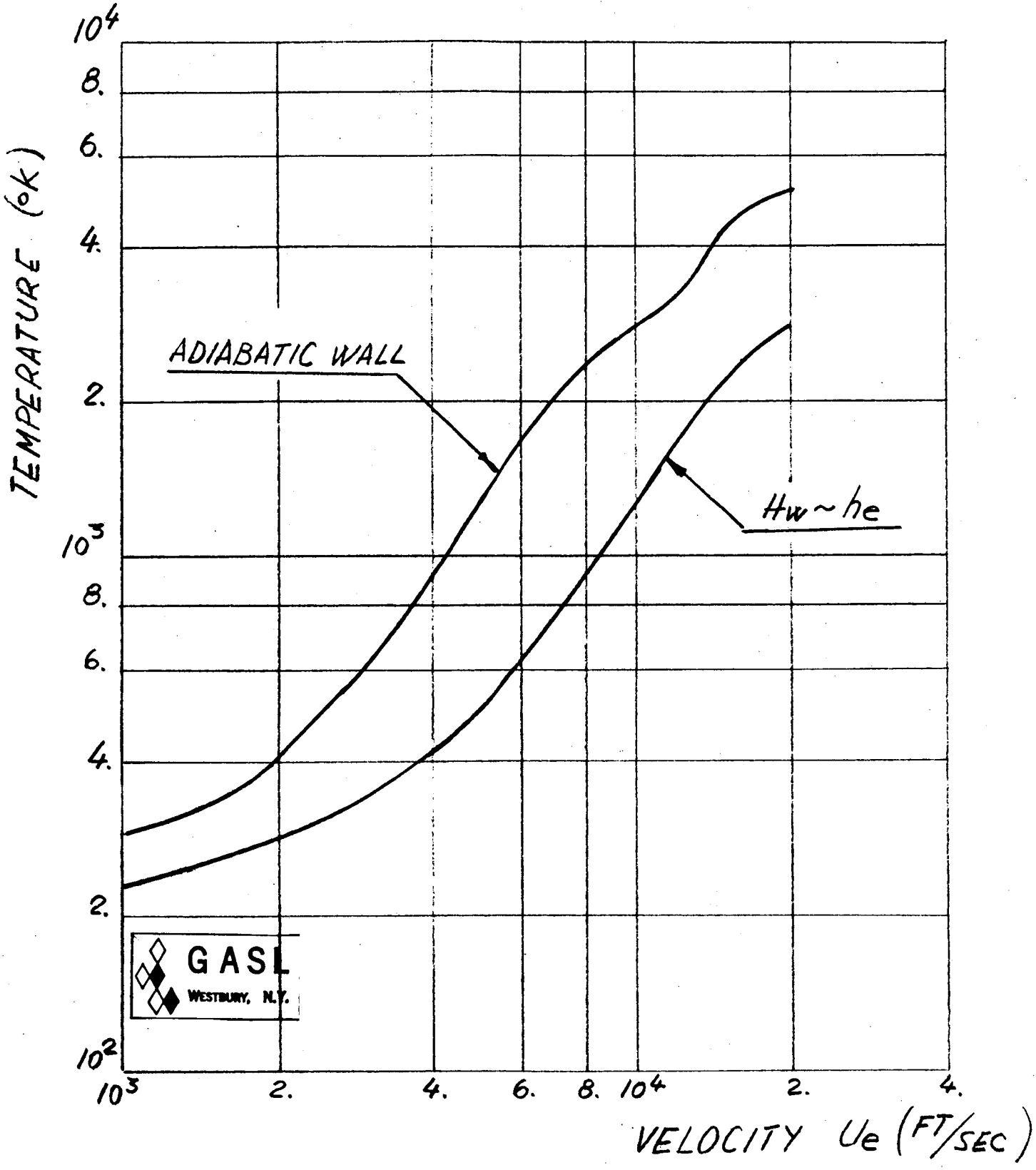

FIG. 3: MAXIMUM STATIC TEMPERATURE IN THE BOUNDARY LAYER _ ALT: 100000 FT.

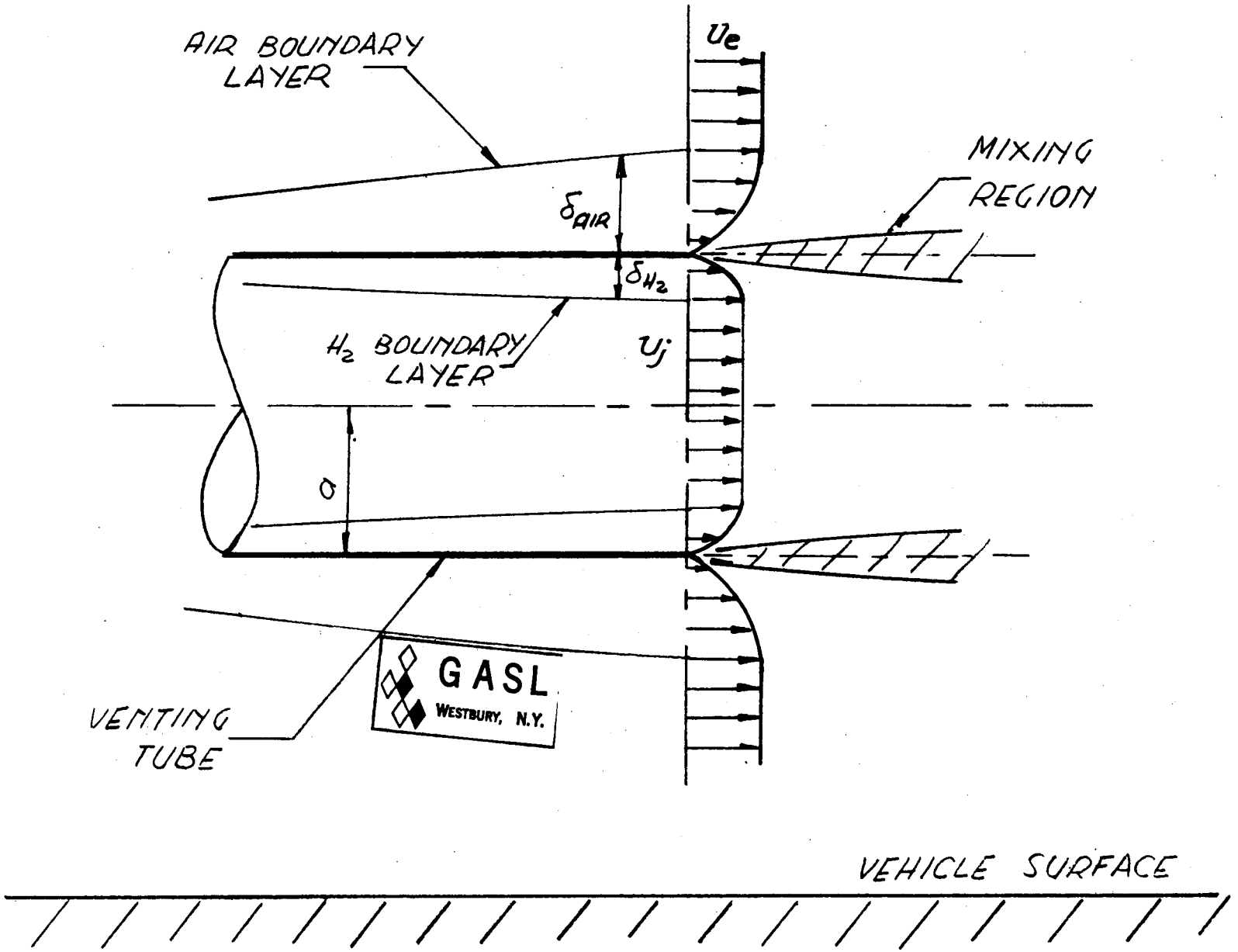

FIG. 4 : SCHEMATIC REPRESENTATION OF THE FLOW FIELD.

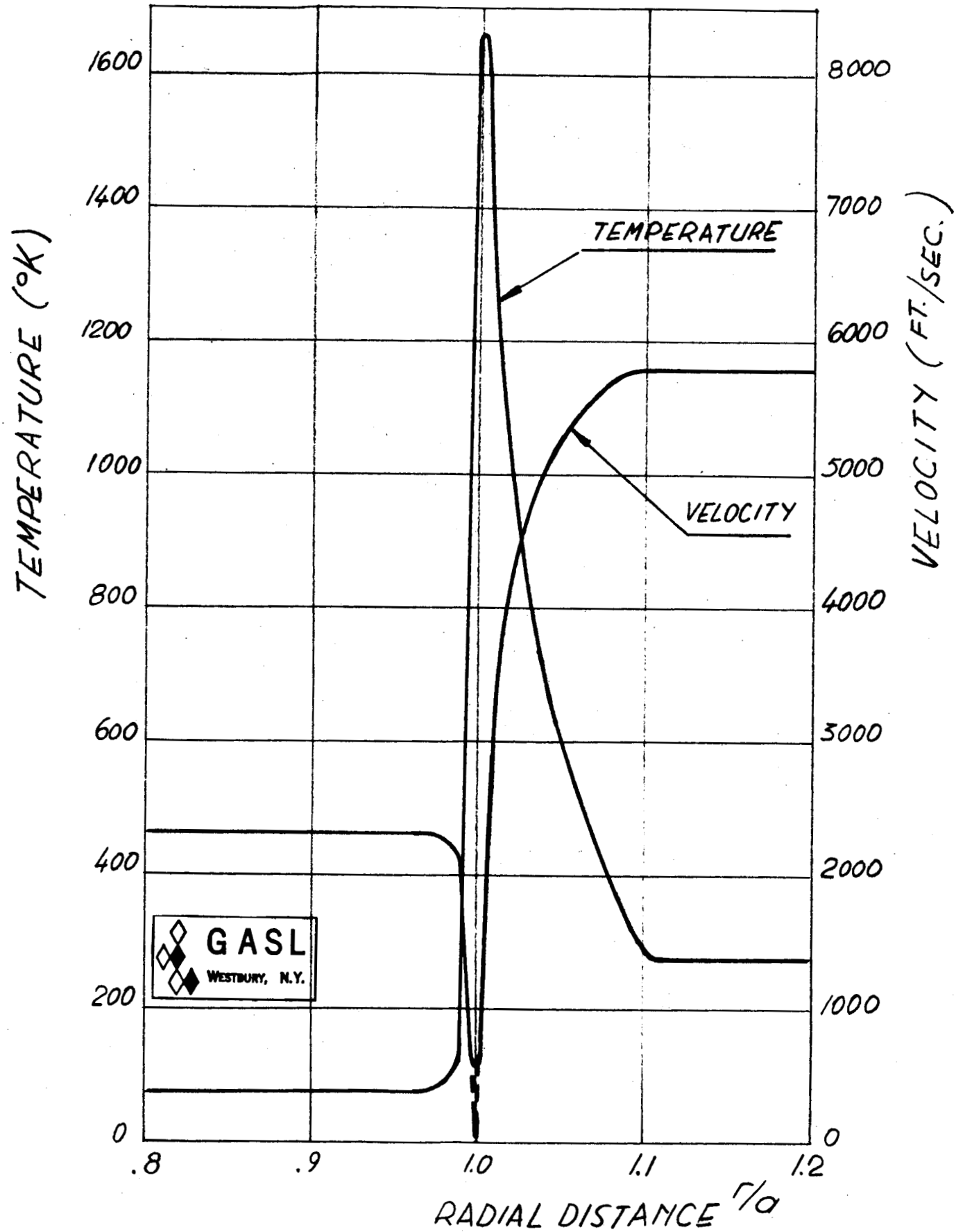

FIG. 5 : VELOCITY AND TEMPERATURE DISTRIBUTION AT INITIAL STATION

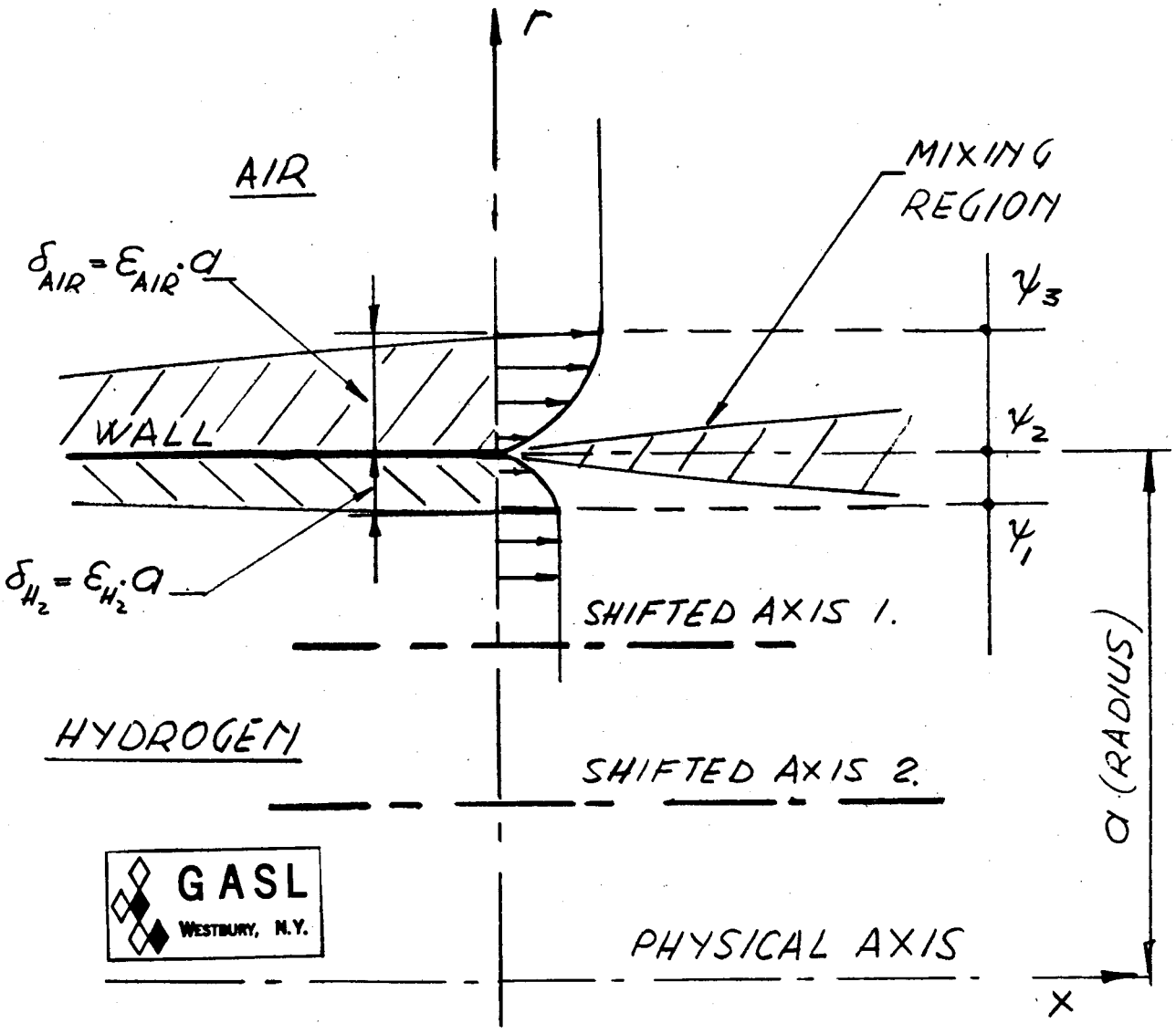

FIG. 6: "SHIFTING AXIS" TECHNIQUE

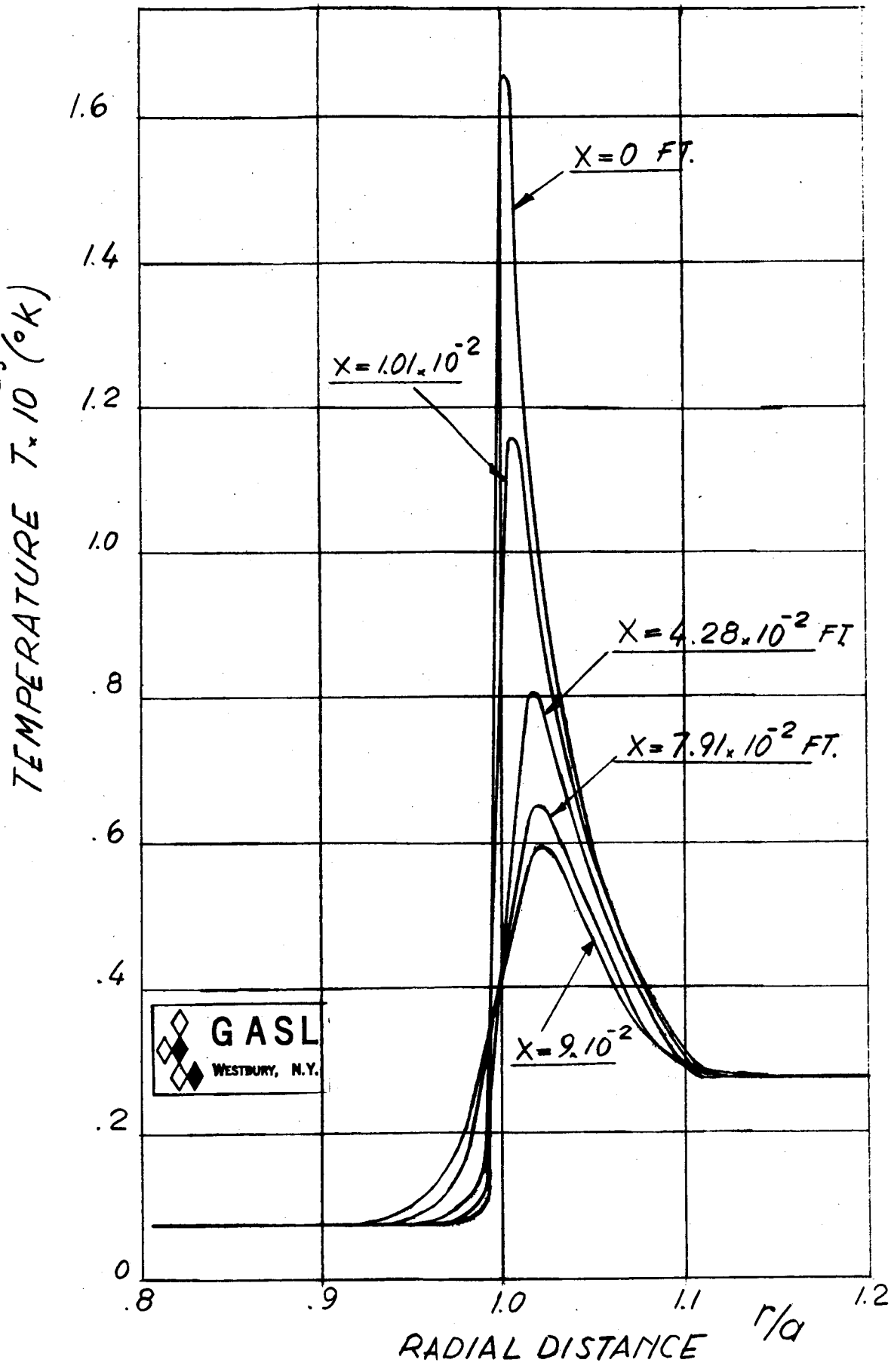

FIG.7 : RADIAL TEMPERATURE DISTRIBUTION

ALT : 50000 FT.

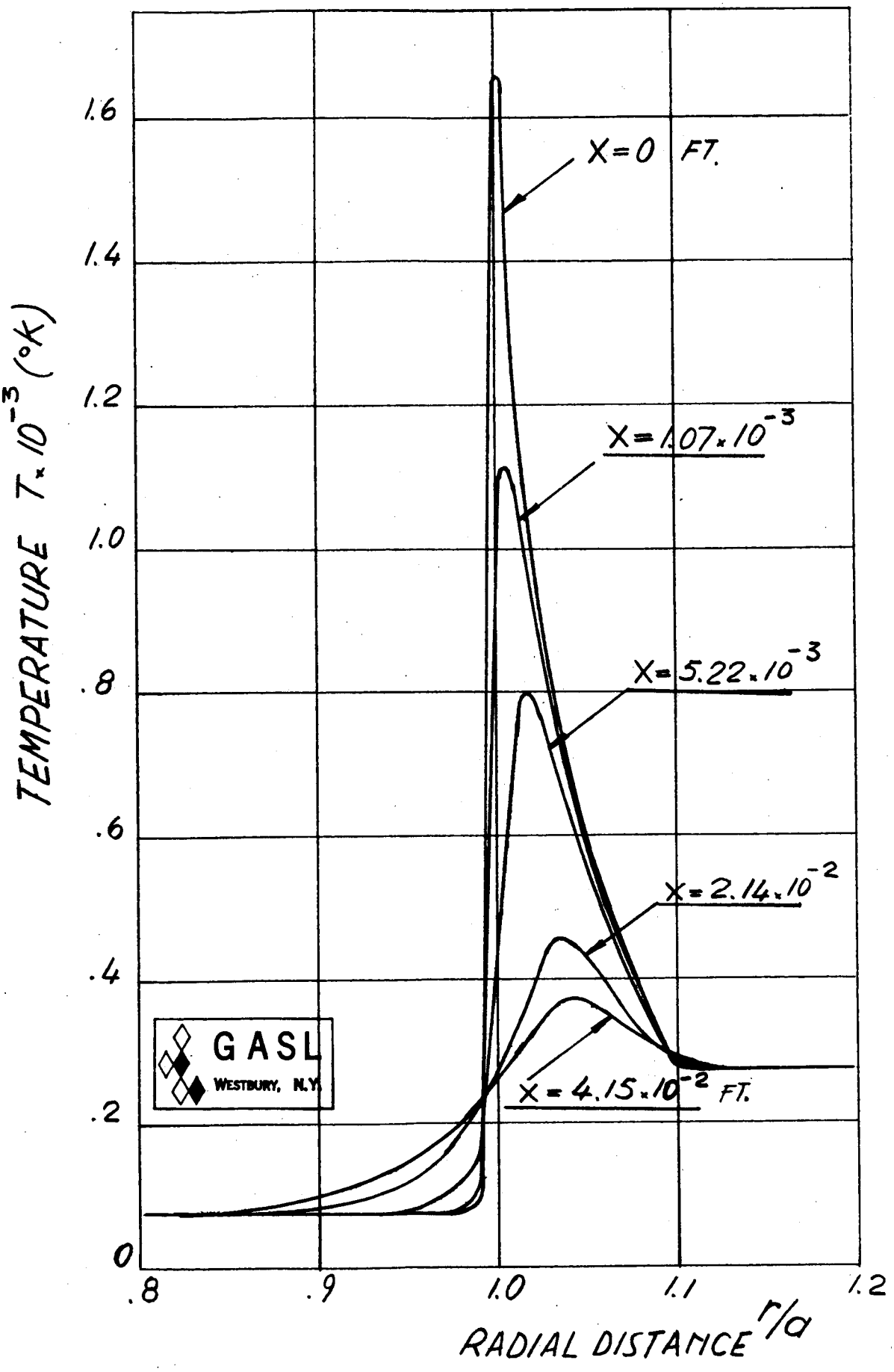

FIG. 8 : RADIAL TEMPERATURE DISTRIBUTION
ALT. 150000 FT.

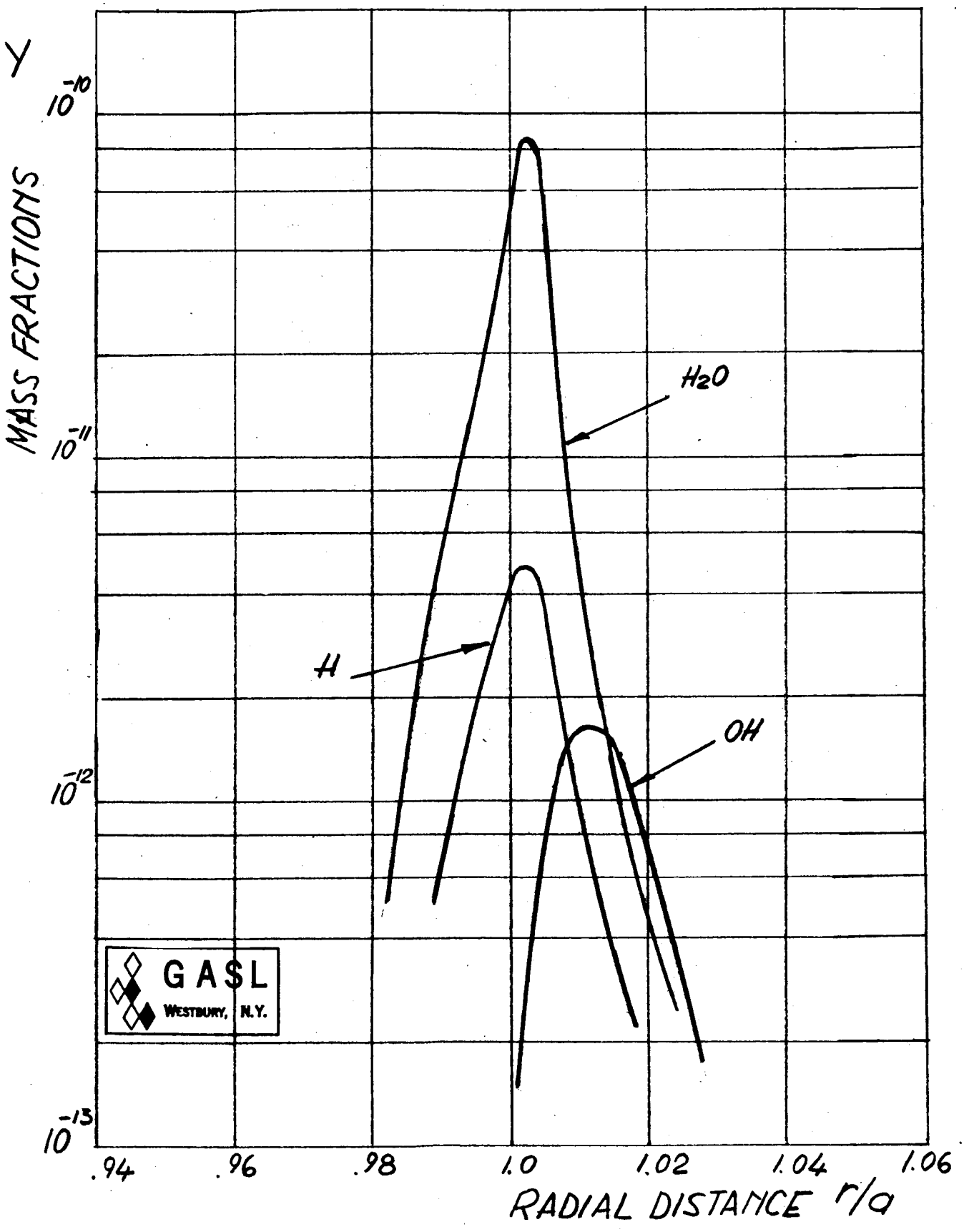

FIG. 9 : TYPICAL MASS FRACTION DISTRIBUTIONS AT $X = 8.10^{-3}$ FT.

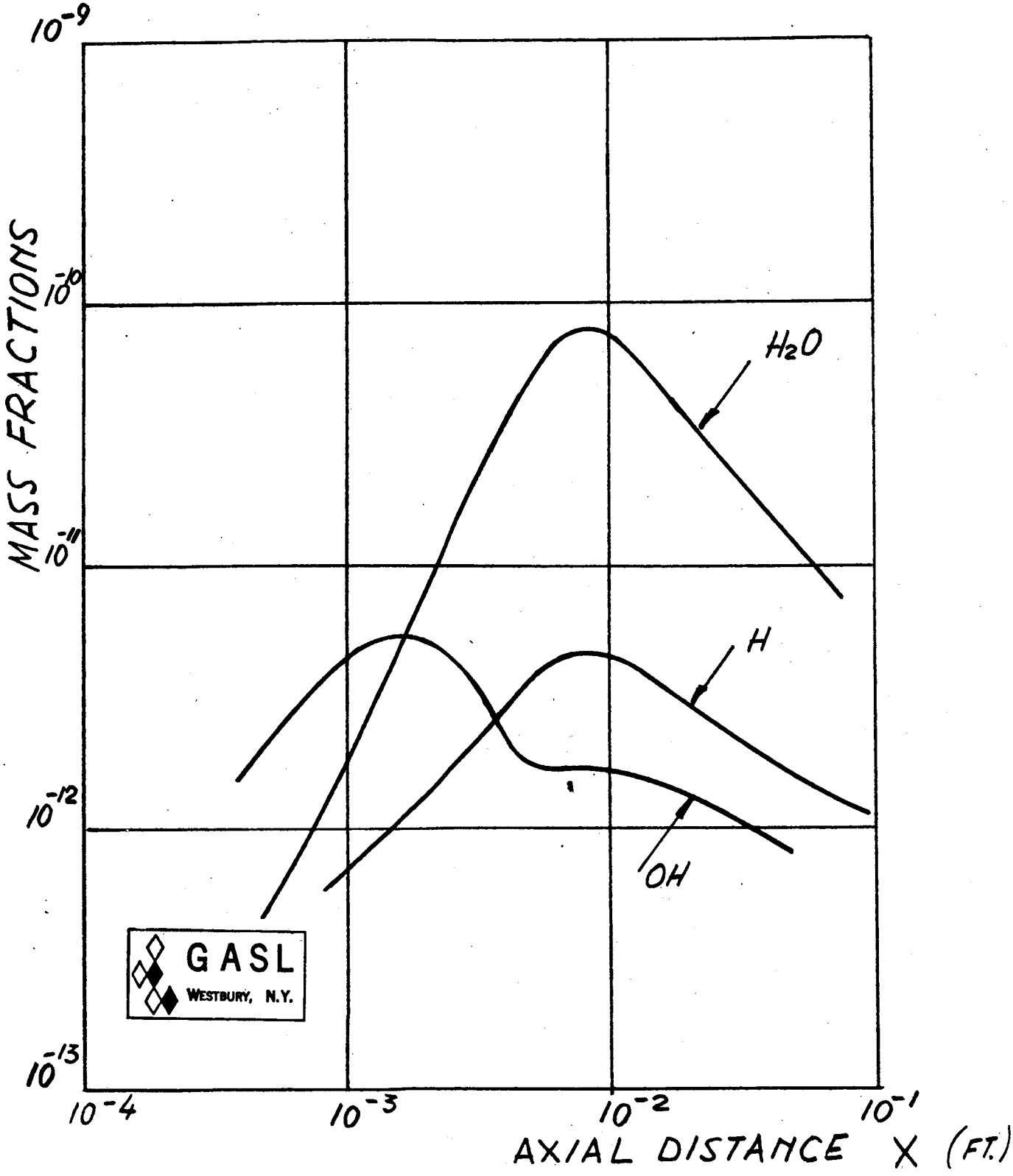

FIG. 10: MAXIMUM VALUES OF H_2O, H AND OH MASS FRACTIONS - ALT. 50000 FT.

Greenstadt, E. W., Ap. J., 145, 270 (1966).

Gringauz, K. I., V. V. Bezrukikh, V. D. Ozerov and R. E. Rybchinskii, Dokl. Akad. Nauk SSSR, 131, 1301 (1960).

Heppner, J. P., N. F. Ness, T. L. Skillman and C. S. Scearce, J. Geophys. Res., 68, 1 (1963).

Hirschberg, J., J. Geophys. Res., 70, 3229 (1965).

Hundhausen, A. J., J. R. Asbridge, S. J. Bame, H. E. Gilbert and I. B. Strong, J. Geophys. Res., 72, 81 (1967a).

Hundhausen, A. J., S. J. Bame and N. F. Ness, J. Geophys. Res., 72, to appear (1967b).

Maer, K. and A. J. Dessler, J. Geophys. Res., 69, 2846 (1964).

McCracken, K. G. and N. F. Ness, J. Geophys. Res., 71, 3315 (1966).

McCracken, K. W., U. R. Rao and N. F. Ness, J. Geophys. Res., 72, to appear (1967).

Ness, N. F. and J. M. Wilcox, Phys. Rev. Letters, 15, 461 (1964).

Ness, N. F. and J. M. Wilcox, Science, 148, 1592 (1965).

Ness, N. F., and J. M. Wilcox, Solar Physics, 1, to appear (1967).

Ness, N. F., C. S. Scearce and J. B. Seek, J. Geophys. Res., 69, 3531, (1964).

Ness, N. F., C. S. Scearce and S. C. Cantarano, J. Geophys. Res., 71, 3305, (1966).

Ness, N. F., J. Geophys. Res., 71, 3319 (1966).

Neugebauer, M. and C. W. Snyder, J. Geophys. Res., 71, 4469, (1966).

Newton, H. W. and M. L. Nunn, MNRAS 111, 413 (1951).

Ogilvie, K. W., T. Wilkerson and N. McIlwraith, GSFC preprint X612-67-330. January 1967.

REFERENCES

Bonetti, A., H. S. Bridge, A. J. Lazarus, E. F. Lyon, B. Rossi and F. Scherb, J. Geophys. Res. 68, 4017 (1963).

Brandt, J. C., M. J. S. Belton and M. W. Stephens, Astron. J., 71, 157 (1966).

Brandt, J. C., Ap. J., 144, 1221 (1966).

Bridge, H. S., A. Egidi, A. Lazarus, E. Lyon and L. Jacobson, Space Res. V, 969 (1965).

Burlaga, L. F. and N. F. Ness, GSFC Preprint X612-67-278, (1967).

Cahill, L. J., Jr. and P. C. Amazeen, J. Geophys. Res., 68, 1835 (1963).

Coleman, P. J., Jr., L. Davis and C. P. Sonett, Phys. Rev. Letters, 5, 43 (1960).

Coleman, P. J., Jr., J. Geophys. Res., 71, 5509 (1966).

Coleman, P. J., Jr., L. Davis, E. J. Smith and D. E. Jones, J. Geophys. Res., 72, 1637 (1967).

Davis, L. J., Jr., E. J. Smith, P. J. Coleman, Jr. and C. P. Sonett, in The Solar Wind, edited by R. J. Mackin, Jr. and M. Neugebauer, pp 35-52, Pergamon Press, New York, 1966.

Dessler, A. J. and J. A. Fejer, Planet. Space Sci., 11, 505 (1963).

Dessler, A. J., Revs. Geophys., 5, 1 (1967).

Dungey, J. W., Phys. Rev. Letters, 6, 47 (1961).

Fairfield, D. H. and L. J. Cahill, J. Geophys. Res., 71, 155, (1966).

Fairfield, D. H. and N. F. Ness, J. Geophys. Res., 72, 2379 (1967).

Fairfield, D. H., NASA-GSFC Preprint X 612-67-174.

Fan, C. Y., G. Gloeckler and J. A. Simpson, J. Geophys. Res., 71, 1837 (1965).